PHILOSOPHICAL TRANSACTIONS OF THE ROYAL SOCIETY A MATHEMATICAL, PHYSICAL & ENGINEERING SCIENCES

Modelling Intraseasonal and Interannual Variability in the Tropics [and Discussion]

M. K. Davey, G. Budin and D. E. Harrison

Phil. Trans. R. Soc. Lond. A 1989 **329**, 155-166
doi: 10.1098/rsta.1989.0067

Phil. Trans. R. Soc. Lond. A **329**, 155–166 (1989)
Printed in Great Britain

Modelling intraseasonal and interannual variability in the tropics

By M. K. Davey and G. Budin

Meteorological Office Unit, Hooke Institute for Atmospheric Research, Clarendon Laboratory, University of Oxford, Parks Road, Oxford OX1 3PU, U.K.

A tropical ocean–atmosphere model of intermediate complexity, incorporating a limited set of physical processes, is used to investigate variability up to interannual timescales. The model atmosphere has a single vertical mode and an explicit moisture budget, whereas the ocean has one active upper layer. Basic experiments confined to a Pacific-size closed ocean basin and the overlying atmosphere are described. Eastward-propagating coupled waves with a period of about six years arise for strong coupling, but with weak coupling a steady equilibrium is reached.

The model has no internal high-frequency variability, so for some cases a small amount of noise is added to the atmospheric forcing terms. This noise is selectively amplified by moist processes in the atmosphere to generate eastward-propagating intraseasonal waves. It is found that these waves have little effect on the robust interannual coupled wave: rather, the interannual mode imposes large-scale patterns that inhibit the intraseasonal waves.

1. Introduction

The principal interannual signal in the tropical oceans and atmosphere is the recurring series of El Niño Southern Oscillation (ENSO) events, of which the very strong 1982–83 and weaker 1986–87 events are the most recent examples. These irregular episodes involve closely linked and substantial changes in the patterns of atmospheric winds, precipitation and pressure, and in oceanic sea level, currents and temperature: see Cane (1986) for a general review. Present and recent tropical conditions are described in the monthly bulletin of the Climate Analysis Centre (1988).

Another major low-frequency signal found principally in the atmosphere is that of intraseasonal waves, with a period ranging from 30 to 60 days, involving both eastward-propagating waves and northward-propagating regional features. This activity is also irregular, and fluctuates in a manner partly related to ENSO events as described by Mehta & Krishnamurti (1988), Lau & Chan (1988), and Gray (1988). The phenomena on both timescales share the property that deep convection and associated latent heat release is an important ingredient of their dynamical behaviour. The question arises as to whether the intraseasonal waves can act as causes of ENSO events under the right circumstances, as hypothesized by Lau & Chan (1986). For example, could the passage of an intraseasonal wave over the western Pacific region at a time of high ocean heat content shift the usual Indonesian convection eastward toward the central Pacific, to in turn trigger coupled growth and development on the interannual scale?

A related tropical feature occurring on a timescale of a few days is the 'westerly burst', which is a sudden outbreak of westerly equatorial winds that frequently occurs in the western Pacific, often associated with near-equatorial cyclones (Keen 1982; Gao *et al.* 1988) and intraseasonal waves (Lau *et al.* 1989). Such a burst was accompanied by a sudden change in the western

Pacific convection and circulation patterns in November 1986 (Nitta & Motoki 1987), at the onset of the 1986–1987 ENSO event. The oceanic response to an earlier burst in May 1986 was observed in detail: the local sea-level change in the western Pacific travelled eastward as a Kelvin wave to be later detected in the central and eastern Pacific (McPhaden *et al.* 1988). However, there did not seem to be a significant sea surface temperature (SST) change associated with this earlier event.

It is not clear whether the westerly bursts or the intraseasonal waves or both can act as triggers for ENSO (either individually or collectively), or are merely modified passively by ENSO events arising from other causes. Coupled models show that ENSO events may recur without invoking such initiators, either through the interaction of local growth with equatorially trapped low-frequency waves in the ocean (Cane & Zebiak 1985; Schopf & Suarez 1988), or as propagating coupled waves intrinsic to the ocean–atmosphere system (Anderson & McCreary 1985; Hirst 1988).

As a first step to investigating the interaction of intraseasonal and interannual waves, we describe here some results from an intermediate tropical ocean–atmosphere model that has a reduced set of dynamics and highly parametrized thermodynamics. The domain of the model is restricted to a Pacific-size rectangular ocean plus the overlying atmosphere. Forcing may include a high-frequency random component to represent variability that is not intrinsic to the model. Two control cases with no random forcing are first presented in §3: in one, interannual waves arise, but in the other, with weaker ocean–atmosphere coupling, a steady state is reached. In either case intraseasonal activity is negligible.

When a small amount of random forcing is added to the atmosphere it is selectively amplified by moist processes, generating mainly Kelvin-like eastward propagating waves, with a timescale of a few days in this Pacific-size model. These waves have little effect on the coupled interannual mode, or on the steady equilibrium state.

2. Description of the model

A brief outline of the basic equations is provided in this section: for a more complete description see Anderson & McCreary (1985) for the ocean, and Davey & Gill (1987) for the atmosphere. The domain for this model spans 168° of longitude and from about 30° N to 30° S. The ocean has $1° \times 1°$ latitude–longitude resolution and a three-hour time step, whereas the atmosphere has $4° \times 4°$ resolution and a time step of 20 min, both on a C-grid. Extra damping at the northern and southern ocean boundaries is provided to eliminate coastal Kelvin waves. The ocean and atmosphere exchange information once per model day.

(*a*) *Oceanic component*

The tropical ocean is represented by a single active layer with depth h and temperature T overlying a passive deep layer with constant temperature T_0 and density ρ_0. In flux form, the horizontal nonlinear equations of motion for the active layer on an equatorial β-plane are

$$(hu)_t + \nabla\cdot(hu\boldsymbol{u}) - fhv = (X - P_x)/\rho_0 + \nu_0\nabla^2(hu), \tag{2.1a}$$

$$(hv)_t + \nabla\cdot(hv\boldsymbol{u}) + fhu = (Y - P_y)/\rho_0 + \nu_0\nabla^2(hv), \tag{2.1b}$$

where $\boldsymbol{u} = (u, v)$ is horizontal velocity, $P = \frac{1}{2}\rho_0 \alpha g h^2 (T - T_o)$ is potential energy, and $f = \beta y$ is the Coriolis parameter. The wind stress is

$$(X, Y) = D(U, V), \tag{2.2}$$

proportional to the surface wind $\boldsymbol{U}$.

Temperature and depth vary according to

$$T_t + \boldsymbol{u}\cdot\nabla T = -2[\gamma(T - T^*) + \delta_0/h^2]/h + \nu_0 \nabla^2 T, \tag{2.3}$$

$$h_t + \nabla\cdot(h\boldsymbol{u}) = [\gamma(T - T^*) + 2\delta_0/h^2]/(T - T_0) - \omega_0. \tag{2.4}$$

The term $\gamma(T - T^*)$ is a Haney-type heat flux representing the net effect of solar input, and evaporative, sensible and radiative cooling. The effective temperature T^* (always larger than T) is constant in time, with the form

$$T^* = 30.6 - 7.9 \sin^2 (\pi y/2y_0), \tag{2.5}$$

which is the largest at the Equator and decreases to the boundaries at $y = \pm y_0$. The term involving the constant δ_0 represents wind mixing that tends to deepen and cool the upper layer, whereas ω_0 is a constant background upwelling that counteracts the deepening and also provides a heat sink to offset the surface heat input. The various constants are listed in table 1. Note that for a depth of 100 m the timescale for temperature change by the Haney forcing is about 200 days.

TABLE 1. PARAMETERS FOR THE MODEL OCEAN

parameter	value	unit	parameter	value	unit
D	1.44×10^{-2}	kg m^{-2} s^{-1}	β	2.28×10^{-11}	m^{-1} s^{-1}
g	9.8	m s^{-2}	γ	3×10^{-6}	m s^{-1}
T_0	17	°C	δ_0	2.74×10^{-2}	m^3 K s^{-1}
y_0	3.44×10^6	m	ρ_0	10^3	kg m^{-3}
ω_0	4×10^{-7}	m s^{-1}	ν_0	2×10^4	m^2 s^{-1}
α	2×10^{-4}	K^{-1}			

The oceanic gravity wave speed is

$$c = [\alpha g(T - T_0)\, h]^{\frac{1}{2}}, \tag{2.6}$$

which varies with position and time. A typical value is about 1.4 m s^{-1}. In the absence of motion the ocean reaches thermodynamic equilibrium with temperature $\overline{T}$ and depth $\overline{h}$ given by

$$\overline{T} = T_0 + \gamma(T^* - T_0)/(\gamma + \omega_0), \tag{2.7a}$$

$$\overline{h} = [\delta_0/\omega_0(\overline{T} - T_0)]^{\frac{1}{2}}. \tag{2.7b}$$

For the parameters chosen, $\overline{T}$ ranges from 29 °C at the Equator to 22 °C at $y = \pm y_0$, whereas $\overline{h}$ increases poleward from 75 m to 100 m.

(*b*) *Atmospheric component*

The atmosphere has the vertical structure of a single baroclinic mode, between the sea surface at $z = 0$ to a rigid lid at the tropopause at $z = \pi H$, and has a constant background buoyancy frequency. The linear equations of motion are

$$U_t - fV = -p_x/\rho_{00} - \epsilon U + \nu_a \nabla^2 U, \tag{2.8a}$$

$$V_t + fU = -p_y/\rho_{00} - \epsilon V + \nu_a \nabla^2 V, \tag{2.8b}$$

when p is the surface pressure perturbation. The constants ϵ etc. are provided in table 2. The mid-level potential temperature perturbation θ is controlled by

$$\theta_t + W(\theta_z)_{00} = \epsilon(\theta_s + \theta_R - \theta) + \nu_a \nabla^2 \theta + mPr, \tag{2.9}$$

where $(\theta_z)_{00}$ is the constant background potential temperature gradient scale. The mid-level vertical velocity W is related to the low-level wind by

$$U_x + V_y + W/H = 0. \tag{2.10}$$

The term θ_s represents heating directly related to the underlying sea surface temperature T, with

$$\theta_s = T - 26.5, \tag{2.11}$$

and θ_R is an additional random heating that may be added to represent processes not explicitly included in the model. Latent heating is included in the form mPr, where Pr is a precipitation rate (see below) and m is a constant conversion factor. The link between (2.8) and (2.9) is that p is related to θ by

$$p/\rho_{00} = -gH\theta/\theta_{00}. \tag{2.12}$$

In this system the speed of a dry gravity wave is

$$C = [g(\theta_z)_{00}/\theta_{00}]^{\frac{1}{2}} H, \tag{2.13}$$

which is about 60 m s^{-1} for the atmospheric parameters listed in table 2.

TABLE 2. PARAMETERS FOR THE MODEL ATMOSPHERE

parameter	value	unit	parameter	value	unit
E_0	10^{-6}	s^{-1}	ϵ	4.4×10^{-6}	s^{-1}
E_v	4×10^{-7}	m^{-1}	θ_{00}	310	K
H	$17000/\pi$	m	$(\theta_z)_{00}$	3.89×10^{-3}	K m^{-1}
m	235	K m^{-1}	ρ_{00}	1.225	kg m^{-3}
q_s (27)	6.8×10^{-2}	m	ν_a	10^5	m^2 s^{-1}

The precipitation rate is determined by a moisture budget whereby changes are partitioned between Pr and column moisture q according to

$$q_t = (1-\sigma)R, \quad Pr = \sigma R \tag{2.14}$$

where

$$R = -\nabla \cdot (Uq) + E + \nu_a \nabla^2 q$$

and

$$\sigma = \begin{cases} (q - q_c)/(q_s - q_c) & \text{if } R > 0 \text{ and } q > q_c, \\ 0 & \text{otherwise.} \end{cases}$$

Here $$q_s = q_s\,(27)\,\exp\{0.06(T-27)\}. \tag{2.15}$$

The threshold value for the onset of precipitation is $q_c = 0.8\,q_s$. Evaporation E depends on wind speed, with

$$E = (E_0 + E_v|U|)\begin{cases} q_s - q & \text{if } q < q_c, \\ q_s - q_c & \text{if } q > q_c. \end{cases} \tag{2.16}$$

The latent heating effectively reduces the atmospheric static stability, and hence reduces wave speeds. For saturation conditions over a sea surface with $T = 27$ °C, wave speeds are approximately halved in this model.

3. Coupled control experiments

Two control experiments, with no random forcing, will be described in this section. In each case the ocean is initially at rest with upper layer temperature $\overline{T}$ and depth $\overline{h}$, while the atmosphere is first allowed to come to equilibrium with the sea surface temperature $\overline{T}$. Because the ocean is bounded on all sides this zonally symmetric initial state quickly becomes asymmetric after the ocean and atmosphere are coupled.

(*a*) *Interannual wave control* (IC)

The coupled model as described in §2 was integrated for 20 model years. An eastward-propagating coupled wave quickly appears and settles into a recurring pattern with a period of about 6.4 years, as can be seen in the time–longitude maps along 2° N in figure 1. During each cycle a patch with warm SST develops in the west 'Pacific' and moves slowly eastward, accompanied by intense precipitation. There is little change in amplitude while crossing the 'Pacific'. The warm patch then lingers near the eastern boundary, maintained by westerly winds in the east 'Pacific', while a new western patch forms. (Note that in this 'Pacific'-only system, with no intervening land, the eastern and western boundaries are effectively adjacent because cyclic boundary conditions are used for the atmosphere.) Cross sections of several oceanic and atmospheric variables are provided in figure 2 for a time when the wave peak is in mid-ocean, to show that the region of warm SST is associated with larger h, eastward currents, lower surface pressure, and winds directed into the region of heavy rainfall. The general structure of the interannual wave is similar to that described previously by Anderson & McCreary (1985) and Hirst (1988); i.e. like a slow oceanic Kelvin wave with the atmosphere effectively in equilibrium with the SST at all times.

(*b*) *No interannual wave control* (NC)

The model was also integrated for 10 years with the direct coupling of the atmosphere to the ocean reduced by a factor of four: i.e. θ_s in equation 2.9 is replaced by $\frac{1}{4}\theta_s$. In this case a steady equilibrium is reached after about four years, with no tendency to produce coupled waves. The final state is summarized by the cross sections along 2° N provided in figure 3. The circulation is much weaker than in the IC case, particularly near the Equator. The light winds drive weak ocean currents, so the upper-layer depth and temperature have little zonal gradient, except near the eastern boundary. Correspondingly, the precipitation pattern remains as an unbroken equatorial strip and the zonal pressure gradient is weak.

PHILOSOPHICAL TRANSACTIONS OF THE ROYAL SOCIETY A MATHEMATICAL, PHYSICAL & ENGINEERING SCIENCES

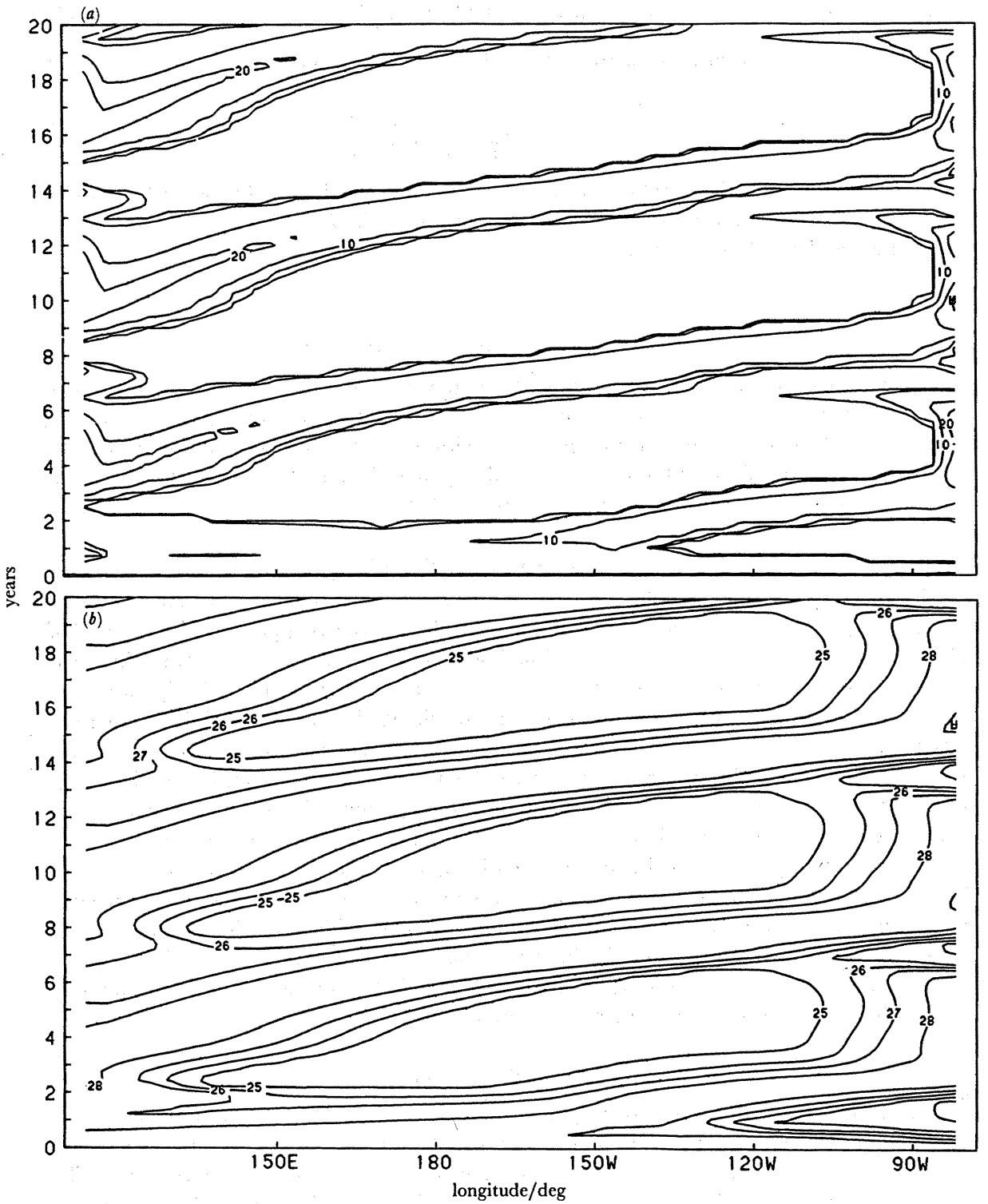

FIGURE 1. Time–longitude sections along 2° N for the interannual wave control (IC) case. (*a*) Precipitation, with contours at 0.1, 1, 10, 20 and 30 mm d^{-1}. Minimum is 0, maximum 32.5. (*b*) Sea surface temperature with contours at integer values. Minimum is 23.8, maximum 29.1.

PHILOSOPHICAL TRANSACTIONS OF THE ROYAL SOCIETY A MATHEMATICAL, PHYSICAL & ENGINEERING SCIENCES

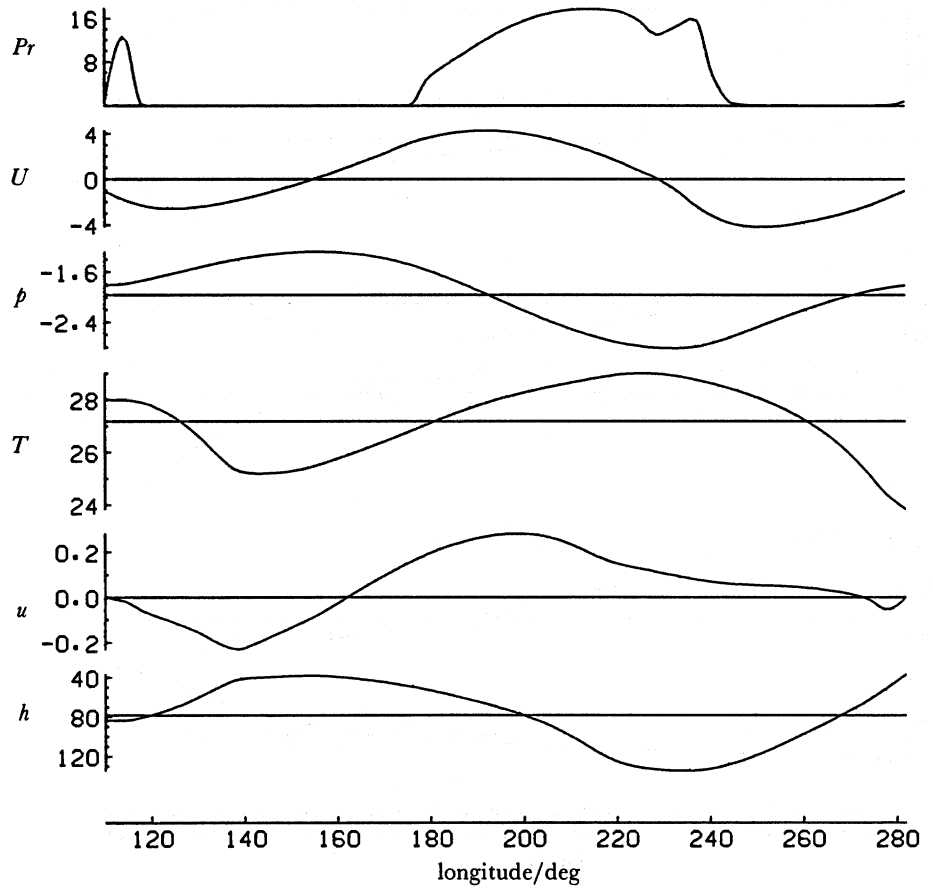

FIGURE 2. Sections along 2° N at the end of year 14 for the interannual wave control (IC) case. Horizontal axes for the surface pressure perturbation p (in millibars, where 1 mbar = 10^2 Pa), upper ocean temperature T and depth h are positioned at the average values.

4. EXPERIMENTS WITH RANDOM FORCING

The control cases contain negligible intrinsic high-frequency variability. To perturb these cases an additional forcing was added to the atmosphere in the form of a fluctuating temperature

$$\theta_R = [1-y/y_0)^2]\, A \sum_{k=1}^{2} \sum_{\substack{n=-9 \\ \neq 0}}^{9} \cos\,[2\pi(kx/L - nt/\tau + \phi_{kn})] \qquad (4.1)$$

where k and n are zonal and temporal wavenumbers, L is the length of the model domain (168° of longitude), $\tau = 36$ days is the repeat period, and ϕ_{kn} is chosen randomly in the range 0–1. Thus the extra term has a discrete truncated white-noise spectrum covering periods from 4 to 36 days. For the experiments described here the amplitude is $A = 0.26$, giving a peak value for θ_R of 2.8 °C for the particular realization (choice of ϕ) used.

(a) *Atmosphere only and random* (AR)

To demonstrate the effect of this forcing the atmospheric component was integrated with SST fixed at $\bar{T}$. The perturbations due to θ_R cause fluctuations in the moisture convergence, and hence in precipitation. The latent heating fluctuations can be several times larger than θ_R itself,

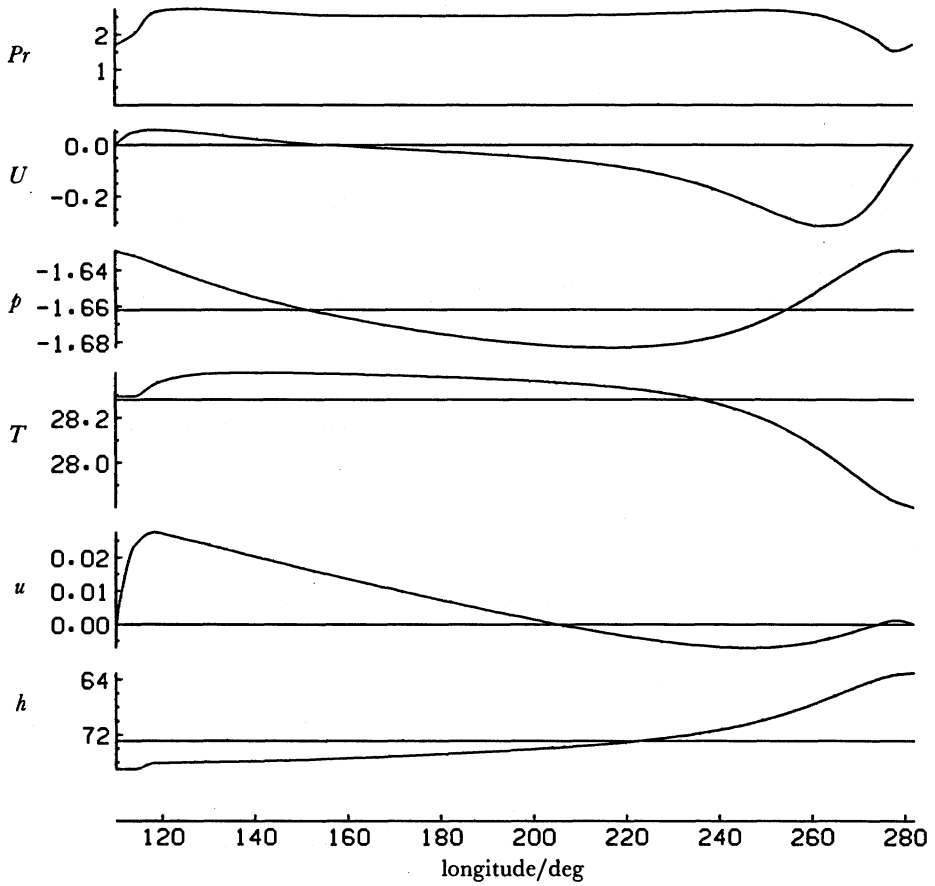

FIGURE 3. Sections along 2° N for the steady state of the no interannual wave control (NC) case. Horizontal axes for the surface pressure perturbation p, upper ocean temperature T and depth h are positioned at the average values.

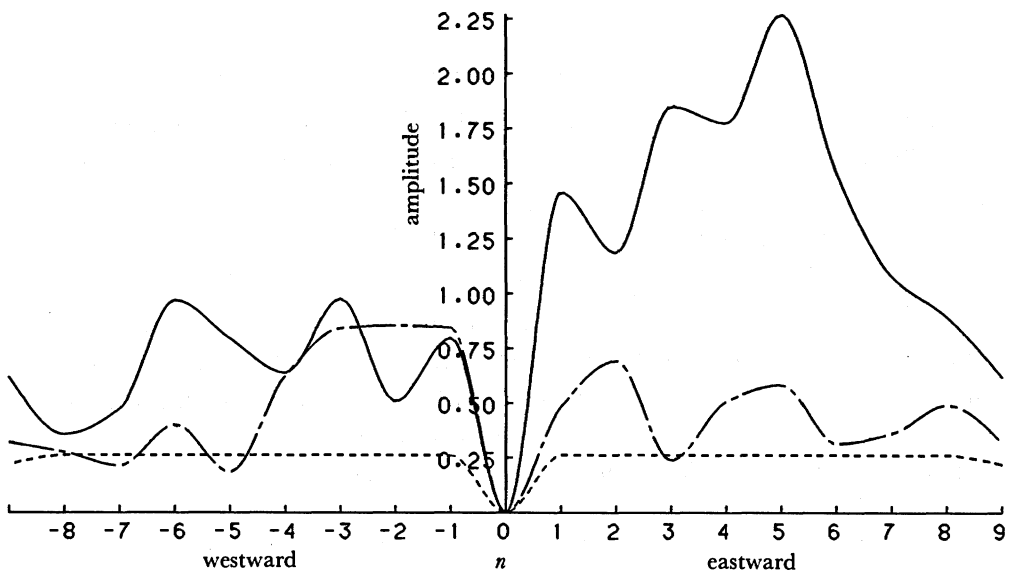

FIGURE 4. Travelling wave amplitude analysis for zonal wave number $k = 1$ for 36 day samples of the random forcing θ_R (short dashes), and mPr/ϵ for the interannual wave (case IR, long dashes) and atmosphere only (case AR, solid) with random forcing. The period of the waves is $36/n$ days.

and become organized to be consistent with the atmospheric circulation that they partly drive. The main response is in the form of eastward-propagating Kelvin waves with zonal wavenumber $k = 1$ and a speed consistent with the gravity wave speed reduced by latent heat release. These features can be seen in figure 4, where travelling wave amplitude spectra of θ_R and mPr/ϵ are provided for $k = 1$ from a 36 day sample. The period for the eastward peak is about 8 days in this Pacific-size domain. Experiments with an atmosphere spanning a full 360° of longitude show the same features with a correspondingly expanded period. The period can be adjusted according to the model parameters chosen: dynamically these waves may correspond to observed intraseasonal waves (Lau & Peng 1987; Davey 1988).

(*b*) *Interannual wave and random* (IR)

Experiment IC was repeated with the random forcing included. The time–longitude section of precipitation along 2° N in figure 5 shows that the interannual wave is not altered significantly by the additional high-frequency variability, neither in its growth stage nor at any time during its regular cycle. Small perturbations are merely superimposed. Other atmospheric variables have similar behaviour, whereas high-frequency disturbances in the ocean are less evident, with SST being the least affected. (The fluctuating winds do cause rapid changes in h and ocean currents, but the ocean thermal timescale is such that SST responds very little to those oscillating changes.)

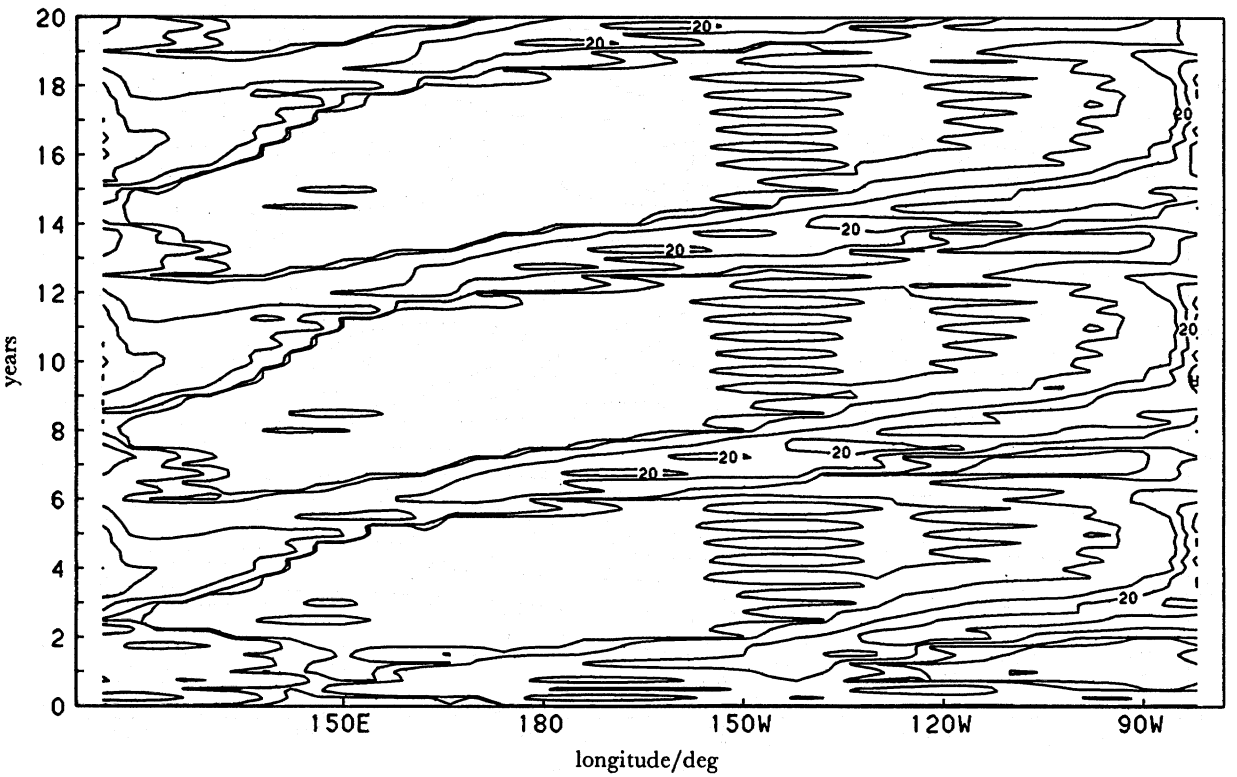

FIGURE 5. Time–longitude section of precipitation along 2° N for the interannual wave case (IR) with random forcing. Contours at 0.1, 1, 10, 20 and 30 mm d^{-1}. Minimum is 0, maximum 35.

PHILOSOPHICAL TRANSACTIONS OF THE ROYAL SOCIETY A MATHEMATICAL, PHYSICAL & ENGINEERING SCIENCES

The interannual wave tends to suppress the atmospheric response to θ_R. Included in figure 4 is the travelling wave spectrum of latent heating from a 36 day sample of the IR experiment, which has a much smaller amplitude than that for the AR case. (The shape of the spectrum is not significant.) The reason for this difference is that the SST pattern due to the coupled interannual wave (which changes relatively slowly) is driving an atmospheric circulation with strong ascent over the warmest SST and descent elsewhere, and this basic circulation inhibits the amplification of θ_R by moist processes.

(*c*) *No interannual wave and random* (NR)

Experiment NC was also repeated with θ_R added. Figure 6 is a time–longitude map of the zonal surface wind field along 2° N for the last 54 days of this case: it shows easterly and westerly bursts of up to 6 m s^{-1}, with a recurrence time of 36 days determined by τ. There is little evidence of eastward propagation in this field, mainly because a large amplitude for θ_R was used. (Clear eastward 'intraseasonal' waves occur for θ_R reduced by a factor of four.) Associated with the strongest westerly burst (about day 8 in figure 6) in the western 'Pacific' there is a weak eastward-propagating deepening of the upper ocean, but there is no noticeable sea surface temperature signal. This lack of SST variability, plus the weak ocean–atmosphere coupling used in this case, means that no slow coupled waves develop and there is no interannual variability.

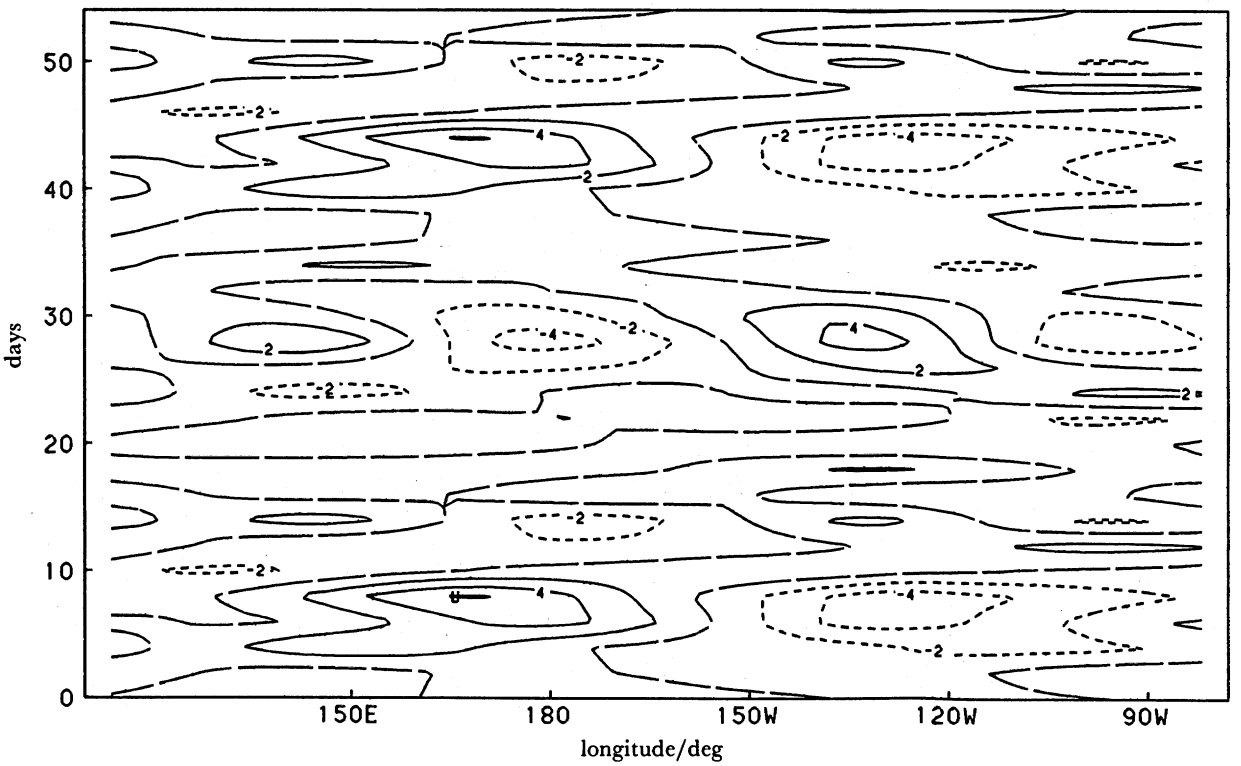

FIGURE 6. Time–longitude section of low-level zonal wind along 2° N for the case with random forcing but no interannual wave (NR). Negative contours broken, positive solid. Minimum is −5.1 m s^{-1}, maximum is 6.1 m s^{-1}.

PHILOSOPHICAL TRANSACTIONS OF THE ROYAL SOCIETY A MATHEMATICAL, PHYSICAL & ENGINEERING SCIENCES

5. Discussion

The model results suggest that it is difficult for short timescale fluctuations to trigger interannual variability in the tropics. The interannual waves depend on ocean–atmosphere coupling, and changes require significant alterations to SST. In the cases described here, high-frequency variability in the atmosphere did not change SST sufficiently to initiate interannual waves, or to disrupt them.

The results should be regarded as preliminary rather than conclusive, however, as they are based on one particular configuration of a particular model. This model has been expanded to include more realistic geometry (Pacific, Indian and Atlantic oceans and intervening land masses), land processes and a seasonal cycle: experiments so far indicate that the interannual mode is then less robust and less regular, and may be more sensitive to shorter timescale variability.

References

Anderson, D. L. T. & McCreary, J. P. 1985 *J. atmos. Sci.* **42**, 615–629.
Cane, M. A. 1986 *A. Rev. Earth planet. Sci.* **14**, 43–70.
Cane, M. A. & Zebiak, S. E. 1985 *Science, Wash.* **228**, 1084–1087.
Climate Analysis Center 1988 *Clim. Diag. Bull.* no. 88/9, 1–25. U.S. Dept. Commerce.
Davey, M. K. 1989 *Q. Jl R. Met. Soc.* (In the press.)
Davey, M. K. & Gill, A. E. 1987 *Q. Jl R. met. Soc.* **113**, 1237–1269.
Gao, S., Wang, J. & Ding, Y. 1988 *Adv. atmos. Sci.* **5**, 87–95.
Gray, B. M. 1988 *J. Climatol.* **8**, 511–519.
Hirst, A. C. 1988 *J. atmos. Sci.* **45**, 830–852.
Keen, R. A. 1982 *Mon. Wea. Rev.* **110**, 1405–1416.
Lau, K.-M. & Chan, P. H. 1986 *Bull. Am. met. Soc.* **67**, 533–534.
Lau, K.-M. & Chan, P. H. 1988 *J. atmos. Sci.* **45**, 506–521.
Lau, K.-M. & Peng, L. 1987 *J. atmos. Sci.* **44**, 950–972.
Lau, K.-M., Peng, L., Sui, C. H. & Nakazawa, T. 1989 *J. met. Soc. Japan* (Submitted.)
McPhaden, M. J., Freitag, H. P., Hayes, S. P., Taft, B. A., Chen, Z. & Wyrtki, K. 1988 *J. geophys. Res.* **93**, 10589–10603.
Mehta, A. V. & Krishnamurti, T. N. 1988 *J. met. Soc. Japan* **66**, 535–548.
Nitta, T. & Motoki, T. 1987 *J. met. Soc. Japan* **65**, 497–506.
Schopf, P. S. & Suarez, M. J. 1988 *J. atmos. Sci.* **45**, 549–566.

Discussion

D. E. Harrison (*NOAA/PMEL, Seattle, U.S.A.*). Ben Giese and I have carried out a number of ocean model studies, using a high spatial resolution version of the Philander and Pacanowski form of the Geophysical Fluid Dynamics Laboratory (GFDL) primitive equation ocean model, of the equatorial response to multi-day episodes of westerly wind in the western equatorial Pacific. We find substantial forcing of both first and second baroclinic mode Kelvin response, and find that as the response propagates into the eastern Pacific with its shallow thermocline the second mode comes to play a major role in the upper ocean current and temperature anomalies. We also find that, although linear equatorial wave theory provides a useful qualitative framework for propagation speeds, the detailed response is substantially different from linear predictions. See Harrison & Giese (1988) for a case study. Thus a ten-day wind episode can produce current and temperature anomalies lasting for well over a month in the eastern Pacific. This process would be excluded *a priori* from any single-mode ocean model like the one you describe.

The data sets of McPhaden *et al.* (1988) to which you refer, which encompasses the May 1986

tropical cyclone pair event that produced strong surface westerly winds in the equatorial western Pacific, can be interpreted as being generally consistent with the results of Harrison & Giese (1988). The observational challenge of observing the oceanic response to such a wind event is considerable, because generally there is both local and remote forcing, because of the possibility of exciting instability waves in the eastern and central Pacific, and because of the complexity of the evolution of the forced response as it propagates through the waveguide current system, as noted by Harrison & Giese (1988). However, much of the observed anomalous surface warming at 110° W appears consistent with remotely forced processes akin to those in the model results of Harrison & Giese (1988).

Reference

Harrison, D. E. & Giese, B. 1988 *Geophys. Res. Lett.* **15**, 804–807.

M. K. Davey. Although the ocean model we used has only a single layer, it is nonlinear and wavespeeds depend on the temperature and depth of that layer so amplification of waves propagating eastward into a cooler, shallower east Pacific region is possible.

The absence of a significant sea surface temperature response to wind bursts in our experiments may be a result of the rather short duration of the anomalous winds produced by the model atmosphere in a truncated Pacific-only domain. Longer bursts would cause larger and more sustained thermocline perturbations which would convert to larger remote SST changes.

PHILOSOPHICAL TRANSACTIONS OF THE ROYAL SOCIETY A MATHEMATICAL, PHYSICAL & ENGINEERING SCIENCES